Available online at www.sciencedirect.com

ScienceDirect

journal homepage: http://www.elsevier.com/locate/acme

Original Research Article

Experimental validation of simulated TB32 crash tests for SP-05/2 barrier on horizontal concave arc without and with composite overlay

Marian Klasztorny [a,*], *Karol Zielonka* [b], *Daniel B. Nycz* [c], *Pawel Posuniak* [b], *Roman K. Romanowski* [d]

[a] *Department of Mechanics and Applied Computer Science, Faculty of Mechanical Engineering, Military University of Technology, 2 gen. S. Kaliskiego Street, PL-00908 Warsaw, Poland*
[b] *Automotive Industry Institute, 55 Jagiellonska Street, PL-03301 Warsaw, Poland*
[c] *Institute of Technology, Jan Grodek State Vocational Academy, 6 Reymonta Street, PL-38500 Sanok, Poland*
[d] *ROMA Co. Ltd., 7 Sloneczna Street, Grabowiec, PL-87124 Zlotoria, Poland*

ARTICLE INFO

Article history:
Received 17 March 2017
Accepted 25 July 2017
Available online 2 November 2017

Keywords:
Road safety barrier on horizontal concave arc
Composite-foam protective overlay
Simulated crash tests
Full-scale experimental crash tests
Experimental validation of numerical modelling and simulation of crash tests

ABSTRACT

The study concerns a selected road safety barrier consisting of a B-type guiderail, Sigma-100 posts with 2.00 m spacing, bolts and supporting elements, located on a horizontal concave arc having a 150 m radius. In order to meet all the functionality criteria, a composite-foam protective overlay is designed and applied. Two full-scale experimental crash tests were carried out, i.e. TB32/CB, TB32/CBC, where TB32 – crash test defined in the EN-1317 standard, CB – curved barrier without the overlay, CBC – curved barrier with the overlay. The numerical modelling and simulation methodology for crash tests, developed by Klasztorny et al. (2016), is applied. Simulations of the above tests were performed using LS-Dyna v.971 finite element code. All the functionality parameters for the barrier are studied. The results of the simulated tests were compared with those of the experimental tests also using the RSVVP programme. The experimental validation of the numerical modelling and simulation is rated positively. It was proven that the TB32/CB crash test does not meet the criteria imposed on the vehicle motion in the exit box, and for the TB32/CBC crash test, these criteria are met.

1. Introduction

According to standards [1,2], crash tests certifying road safety barriers are performed experimentally on a straight section of the barrier. The approval criteria for a crash test include the following functionality parameters of the barrier: acceleration severity index ASI, theoretical head impact velocity THIV, working width W, vehicle motion trajectory in the exit box, penetration of the vehicle into the barrier and vice versa, as

* *Corresponding author.*
E-mail addresses: m.klasztorny@gmail.com (M. Klasztorny), k.zielonka@pimot.eu (K. Zielonka), daniel.nycz@interia.pl (D.B. Nycz), p.posuniak@pimot.eu (P. Posuniak), rromanowski@roma.torun.pl (R.K. Romanowski).
http://dx.doi.org/10.1016/j.acme.2017.07.007

well as continuity of the guide rail during the collision. After performing a crash test, it should also be confirmed that the length of the test section of the barrier is sufficient to demonstrate the full operation of the system. This is determined by the side deflection of the barrier, which should not reach the edge sections of the barrier.

Standard [3] introduces the possibility of certification by the simulation of road safety barriers slightly modified in reference to the so-called parent barrier (certified experimentally). It is therefore reasonable to develop numerical modelling and simulations of road crash tests.

Standards [1–3] define crash tests and functionality parameters in reference to rectilinear road safety barriers. In the case of a vehicle collision with a barrier in a horizontal concave arc, located on a road bend, a vehicle may skid (yaw rotation of the car), increase the working width, or reflect from the barrier without fulfilling the exit box criteria. Therefore, it is appropriate to develop simulated and experimental studies towards verification of the above thesis, as well as towards modification of the barrier to approve the standard crash tests.

The literature review on numerical modelling and simulation of road crash tests was done in Ref. [4] including Refs. [5–7]. As for full-scale experimental crash tests, Ren and Vesenjak [5] compared the TB11 crash test with the experimental test. Borovinsek et al. [6] also compared the simulated TB11 and TB42 crash tests with the experimental tests.

Klasztorny et al. [4] examined a SP-05/2 road safety barrier of a N2-W4-A class (producer Stalprodukt JSC, Bochnia), with a B-type guide bar, located on a horizontal concave arc in an accelerated traffic main road, with the allowable radius of the road axis belonging to the range of 140–220 m. In order to ensure approving the TB11 and TB32 crash tests for the barrier located on a horizontal concave arc, a composite-foam overlay (code CFR2) was designed, which was combined with the B-type guide bar with screw connectors using only the empty holes in the guide axis, at 2.00 m intervals. The overlay is flame retardant, resistant to atmospheric factors and required chemicals, increases the flexibility and strength of the barrier and reduces the vehicle–barrier friction.

The study presents the full-scale experimental validation of the numerical modelling and simulation of the TB32/CB and TB32/CBC crash tests, where CB – curved barrier without the overlay, CBC – curved barrier with the CFR2 overlay. The methodology for the numerical modelling and simulation of the TB11 and TB32 crash tests, developed in Ref. [4] and presented in a shortened form in Section 4 is applied in this study.

2. Functionality parameters and criteria of road safety barriers

The functionality parameters and criteria, test methods and action classes in reference to road restraint systems are specified in Refs. [1,2]. Standards [1,2] do not consider road safety barriers on road bends. Based on Refs. [1,2] Klasztorny et al. [4] summarized the restraint levels, the collision intensity levels and the functionality parameters and criteria. In this study, the information relevant in this work is provided below.

In the case of restraint level N2, the approval of TB11 and TB32 crash tests is required. The TB32 crash test conditions are as follows: impact velocity 110 km/h, collision angle 20°, total car mass 1500 kg. The basic functionality parameters are ASI and THIV. The A level corresponds to ASI ≤ 1.0, THIV ≤ 33 km/h. Acceleration severity index ASI(t) is calculated from the formula [1]

$$\mathrm{ASI}(t) = \sqrt{\left(\frac{\overline{a}_x(t)}{\hat{a}_x}\right)^2 + \left(\frac{\overline{a}_y(t)}{\hat{a}_y}\right)^2 + \left(\frac{\overline{a}_z(t)}{\hat{a}_z}\right)^2}, \quad \mathrm{ASI} = \max_t [\mathrm{ASI}(t)] \tag{1}$$

where

$$\overline{a}_j(t) = \frac{1}{\delta}\int_t^{t+\delta} a_j(t)dt, \quad j = x, y, z \tag{2}$$

and: x, y, z – longitudinal, lateral and vertical directions in the vehicle, respectively, t – time variable, $a_x(t)$, $a_y(t)$, $a_z(t)$ – acceleration components related to the car centre-of-gravity, $\hat{a}_x = 12g, \hat{a}_y = 9g, \hat{a}_z = 10g$ – limits of acceleration components in x, y, z-directions, $\overline{a}_x(t), \overline{a}_y(t), \overline{a}_z(t)$ – acceleration components related to the car centre-of-gravity, filtered with a four-pole phaseless Butterworth digital filter, of low-bandwidth, of the filter cut-off frequency of 13 Hz (acceleration component values averaged over a moving time interval $\delta = 50$ ms), $g = 9.81$ m/s^2 – gravity acceleration.

The collision velocity of the theoretical head with the moving theoretical cabin is the THIV parameter [1]. The calculation algorithm for parameter THIV takes into account the longitudinal velocity, lateral velocity and yaw rotational velocity. Standard [2] stands 8 levels of working width; level W4 corresponds to distance W ≤ 1.3 m.

The functionality criteria for the exit box are as follows. The car, after collision with the barrier and shifting in contact with the barrier, should bounce from the barrier so that the wheel trace does not exceed the front line of the exit box, which is located at a distance of A = 2.2 m + the car width + 16% of car length [2]. For Dodge Neon car this distance is A = 4.53 m. The exit box is B = 10 m long, starting from the exit point of last wheel beyond the barrier face original line. Locking the vehicle in the barrier or skidding is permitted. The vehicle cannot roll over during and after the impact.

3. Description of barrier SP-05/2 and composite-foam protective overlay CFR2

A SP-05/2 road safety barrier and the CFR2 overlay are described in detail and illustrated in Ref. [4]. Based on Ref. [4], the critical data on the barrier and overlay, relevant in this study, is provided below.

A SP-05/2 road safety barrier [8] of the N2-W4-A category [2], made of hot-dip galvanized S235JR steel, is produced by Stalprodukt JSC Co., Bochnia, Poland. The connectors use M16 bolt sets of a 4.6 strength class. The main structural components of the barrier are: a B-type guide rail consisting of segments of an overall length of 4.30 m and a 4.00 m

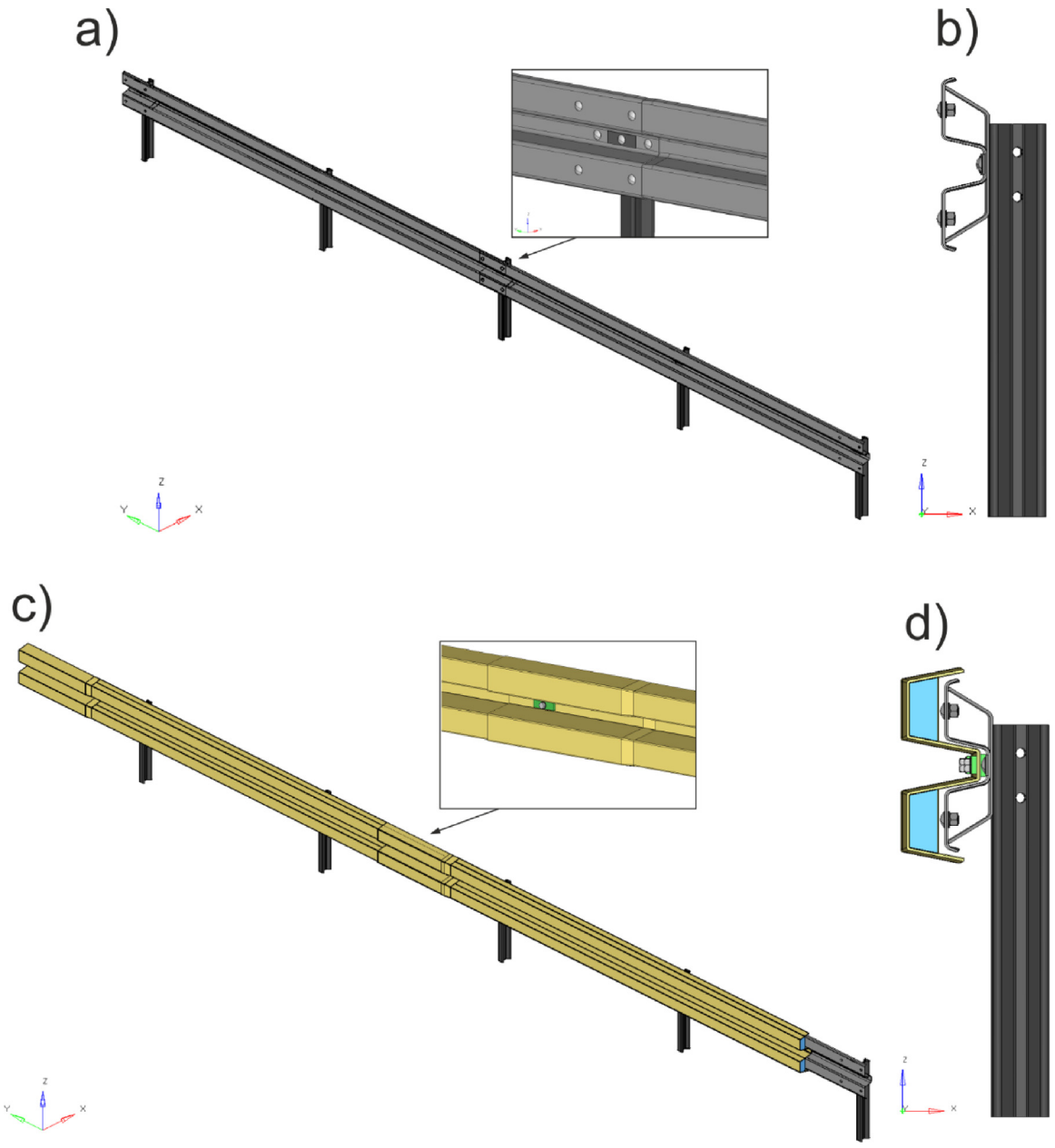

Fig. 1 – Geometrical models of barrier SP-05/2 without and with overlay: (a) two segments of SP-05/2 barrier in isometric view; (b) cross section of SP-05/2 barrier; (c) two segments of CFR2 overlay in isometric view; (d) cross section of SP-05/2 barrier with CFR2 overlay.

effective length, Sigma-100 posts of a length of 1.90 m at intervals of 2.00 m, supporting elements of a trapezoidal cross section and A-type rectangular pads.

Fig. 1 shows the geometrical models of two consecutive segments extracted from a SP-05/2 barrier, of an 8.00 m effective length, without the overlay (Fig. 1a and b) and with the overlay (Fig. 1c and d). The front isometric views are shown in Fig. 1a and c, and the cross-sections in Fig. 1b and d, respectively. The zooms of a guiderail segment connection and an overlay segment connection are also presented in Fig. 1a and c, respectively. Cross sections A–A and B–B and the holes in the overlay segment are presented in Fig. 2.

The overlay is composed of segments of an overall length of 4.70 m and a 4.00 m effective length. The cross section of the overlay is correlated with the cross section of a B-type guide rail including the clearances to cover the horizontal curvature of guide rail B, screw connectors, manufacturing imperfections and thermal deformations. Technological fillet corners with a radius of 5 mm are used. An overlay segment is composed of a prismatic section with a foam insert in two channels of a 3.90 m length, a transition section without filling of a 6 cm length and a prismatic section without filling, overlapping the next segment with a length of 0.74 m.

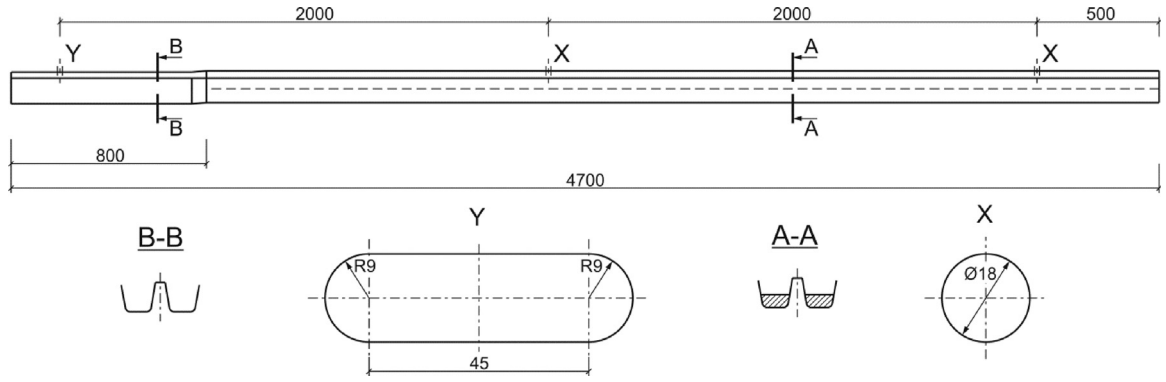

Fig. 2 – Segment of overlay CFR2 – overall dimensions and holes X, Y.

The CFR2 overlay is composed of a GFRP composite front shell, GFRP composite rear shell and polyurethane foam cores in two channels (Fig. 2). The ply sequence in the front shell with a total thickness of 4 mm is as follows: gelcoat, E-glass mat of 450 g/m^2, two layers of E-glass [0/90] plain weave fabric of 600 g/m^2 each, where direction 0 coincides with the barrier axis. The back shell with a total thickness of 1.5 mm, closing the channels, is reinforced with one layer of E-glass mat of 450 g/m^2 and protected with a topcoat. A flame retardant polyester resin is used as the matrix and polyurethane foam of 42 kg/m^3 is applied. The segments and the guide rail are screwed together by means of holes in the guide axis (at 2.00 m intervals), using M16/80 screws of strength class 8.8, using rectangular A-type steel pads and rectangular 70°ShA hardness rubber pads of a thickness of 10 mm. Segments of the CFR2 overlay were manufactured by ROMA Co. Ltd, Grabowiec, Poland, using hand lay-up technology.

4. Shortened description of methodology of numerical modelling and simulation of TB32 crash tests of road safety barriers

The TB32 crash tests were simulated using the non-linear explicit LS-Dyna finite element (FE) code. The Dodge Neon car numerical model was taken from the public library developed by the National Crash Analysis Center, USA (NCAC) [9] and properly corrected [4]. At present, the link given as Ref. [9] is inactive and currently those FE vehicle models are available at the National Highway Traffic Safety Administration, USA website [10].

The vehicle numerical model includes more than 330 material models assigned to particular parts of the car and consists of ~279,700 finite elements. All the functionality parameters and criteria of the tested barrier, specified by standards [1,2], were determined.

The following software was used in the numerical modelling and simulation:

- preprocessing: Catia v5r19 (Part Design, Generative Shape Design, Assembly Design), HyperWorks 11.0 (HyperMesh, HyperMorph), LS-PrePost 4.2
- processing: LS-Dyna v.971
- postprocessing: HyperWorks 11.0 (HyperView, HyperGraph), LS-PrePost 4.2, Excel.

The main items of the numerical modelling and simulation methodology are listed and described in a concise form in Tables 1–4. Original terms, symbols and units, used in the Keyword User's Manual [11], are applied.

5. Experimental crash test technology

Full-scale experimental TB32 crash tests were carried out on the testing grounds at the Automotive Industry Institute, Warsaw, Poland, designed to carry out crash tests on all restraint levels of a protection system. The testing grounds consist of two main parts:

- a drive track 3.2 m wide and 200 m long, equipped with a drive rail, driving ropes, a drive trolley and a drive motor, used to accelerate the vehicle
- a crash square of a 1300 m^2 area (length 55 m, width 25 m).

On the crash square surface, a set of markers was applied allowing analysis of the recording by a video camera placed above the crash site and a tape was stuck to define the exit box for the given crash test. The recording equipment met the requirements specified in standard [1]. The video recording uses three cameras for fast photos (min. 500 frames per second). The cameras were placed in front of and behind the barrier arc. The third camera was placed on an arm at a height of 24 m to record the respective crash site (top view). The impact velocity of the car was measured using a laser device. To ensure safety, concrete barriers and an RC emergency braking system for the test vehicle were installed.

The following measurement equipment was used:

- acceleration sensors – Measurement Specialties model 64C, mounted in the centre of gravity of the vehicle, to measure the acceleration components in the directions of the longitudinal, lateral and vertical axes of the vehicle;
- angular rate sensors – DTS model ARS-8K, mounted in the centre of gravity of the vehicle, to measure the angular rate

Table 1 – Parameters or options of numerical modelling and simulation of road safety barrier crash tests. Part 1.

Item	Parameters/options
Road safety barrier shell steel parts meshing	4-node shell finite elements of QUAD4 topology; Belytschko–Tsai formulation with 1 in-plane integration point and 5 integration points through thickness (ELFORM_2 formulation)
Road safety barrier shell steel parts material model	*MAT_PIECEWISE_LINEAR_PLASTICITY (*MAT_24) elastic-plastic model with isotropic hardening; Material constants taken from manufacturer's certification excluding FAIL parameter; FAIL numerical parameter determined on basis of calibration tests sensitive to meshing (plastic strain to failure and finite element erosion)
6-screw joints of guiderail segments	Discrete beam elements with 6 DOFs, reflected by 6 stiffness characteristics (ELFORM_6 formulation); *NONLINEAR_PLASTIC_DISCRETE_BEAM (*MAT_068) nonlinear elastoplastic and linear viscous model; Parameters and stiffness characteristics determined by comparison of 3D and 2D tension test modelling of guiderail joint section; 3D modelling: • 8-node solid elements of HEX8 topology • constant stress solid element (ELFORM_1 formulation) • Flanagan–Belytschko stiffness form of hourglass control
Guiderail – post screw joints	*CONSTRAINED_GENERALIZED_WELD_SPOT kinematic constraints; Load capacities taken from bolt characteristics
Screw preload	Dynamic relaxation procedure and *INITIAL_STRESS_SECTION option; Approach used in 3D modelling only
Asphalt/concrete pavement surface; Roadside surface	Rigid horizontal plane
Road side soil meshing	Posts embedded in soil cylinders; 3D finite elements of HEX8 and PENTA6 topology; 8-node solid element, trilinear shape functions, 1 integration point (ELFORM_1 formulation)

components around the longitudinal, lateral and vertical axes of the vehicle;
- DTS recording system to record with sampling rates up to 100 kHz;
- laser device to measure the impact velocity of the car (at a distance of 15 m from the barrier);
- 3 Phantom cameras for fast photos.

The location of the centre-of-gravity of the test car was examined in the Laboratory of Testing Vehicles, Automotive Industry Institute, Warsaw, Poland, according to standard [12]. With respect to full-scale experimental crash tests, the conditions specified by standards [1,2] were met for testing grounds, test vehicles, test sections of the barrier, position of the vehicle – barrier collision point, recording area of the crash test, crash test course, recorded results and processing of the measurement results.

6. Full-scale experimental verification of modelling and simulation of selected crash tests

6.1. *Description of test sections of barrier without overlay and with overlay and description of crash tests*

Test sections of the SP-05/2 barrier had a length of 64.00 m as measured along the concave arc with a radius of 150 m (Fig. 3). The central part with a length of 40.00 m was composed of 10 segments of guide rail, with a 4.00 m effective length each, and Sigma-100 posts interspaced 2.00 m. Barrier ends with a length of 12.00 m each were mounted horizontally.

In the TB32/CBC crash test, 9 segments of the CFR2 overlay were applied, arranged in accordance with the diagram shown in Fig. 3. It was assumed that the overlay in other sectors of the barrier, far from the vehicle – barrier collision zone, has little effect on the course of the crash test, hence, the overlay segments in those sectors are not used.

The impact angle, as measured between the longitudinal axis of the vehicle and the tangent to the arc of the guide rail at the intersection of the vehicle axis with this arc, was 20°, which corresponds to an angle of 23° between the axis of the drive track and the tangent to the guide arc in the middle of the barrier test section (Fig. 4). The distance of the arc of the mounting the posts from the concrete pavement edge was 0.30 m. The theoretical point of impact, i.e. the intersection of the drive track axis with the guide face arc was located at a distance of 7.00 m from the barrier centre.

The following experimental and simulated crash tests for barrier SP-05/2 mounted on a horizontal concave arc of a R = 150 m radius were conducted:

- test TB32/CB – barrier without an overlay, v_i = 97.7 km/h
- test TB32/CBC – barrier with overlay CFR2, v_i = 103.7 km/h

where v_i – the experimental impact velocity of the car. The simulation included a time interval of 0–3 s measured from the collision start time. As the barrier was located on the arc, the

Table 2 – Parameters or options of numerical modelling and simulation of road safety barrier crash tests. Part 2.

Item	Parameters/options
Road side soil material model	*MAT_SOIL_AND_FOAM (*MAT_005) model; Material constants taken from NCAC library [9]; Soil cylinders coated with artificial shell with properties of *MAT_NULL (*MAT_009) material; No contact with roadside surface
Laminate shell parts meshing	4-node shell finite elements of QUAD4 topology; Belytschko–Tsai formulation with 1 in-plane integration point and 1 integration for each lamina (ELFORM_2 formulation)
Laminate shell parts material model	*MAT_ENHANCED_COMPOSITE_DAMAGE (*MAT_054) linear elastic-brittle model with Chang–Chang failure criterion; elasticity and strength material constants for laminas reinforced with fabrics or mats determined experimentally at room temperature according to respective standards
Polyurethane foam meshing	8-node solid elements of HEX8 topology; Constant stress solid element (ELFORM_1 formulation); Flanagan–Belytschko stiffness form of hourglass control
Polyurethane foam material model	*MAT_HONEYCOMB (*MAT_026) model; Material constants and characteristics determined experimentally at room temperature (taken for reference)
Guiderail – overlay screw joints	Load capacity loss results from laminate damage included in *MAT_54 material model; *CONSTRAINED_GENERALIZED_WELD_SPOT elements; Load capacities taken from bolt characteristics
Rubber pads meshing	8-node solid elements of HEX8 topology; Constant stress solid element (ELFORM_1 formulation); Flanagan–Belytschko stiffness form of hourglass control; Approach used in 3D modelling only
Rubber pads material model	*MAT_MOONEY-RIVLIN_RUBBER (*MAT_027) two-term model; Material constants determined based on σ–ε curve using least square method

Table 3 – Parameters or options of numerical modelling and simulation of road safety barrier crash tests. Part 3.

Item	Parameters/options
Vibration damping	*DAMPING_PART_STIFFNESS damping model; Damping ratios: • road safety barrier shell steel parts: 0.03 • road side soil: 0.10 • rubber pads: 0.90 • laminate parts: 0.10 • polyurethane foam core: 0.15
Car models	Geo Metro and Dodge Neon car numerical models taken from NCAC public library [9]; Corrections to adapt car models to oblique crash tests: • changing tire model from *AIRBAG model into *AIRBAG_SIMPLE_PRESSURE_VOLUME model • declaration of tire pressure equal to 2.3 bar • correction of suspension (application of *MAT_66 material model and BEAM elements in ELFORM_6 formulation, stiffness and damping suspension adjustment, adding preload in dynamic relaxation process) • dynamic relaxation (influence of gravity load) before starting vehicle collision with barrier • declaration of vehicle linear velocity and wheel angular velocity at start time point • adjustment of wheel alignment and wheel rotation axis • correction of contact options • correction of control cards • hourglass control (elimination of non-physical forms of vibration) • placing *ELEMENT_SEATBELT_ACCELEROMETER at car centre of gravity on rigid solid element connected to chassis by means of *CONSTRAINED_EXTRA_NODES bonds • correction of bond stiffness
Contact	*CONTACT_AUTOMATIC_SINGLE_SURFACE model between potential contact pairs; Additionally, *CONTACT_INTERIOR for roadside soil and foam

Table 4 – Parameters or options of numerical modelling and simulation of road safety barrier crash tests. Part 4.

Item	Parameters/options
Friction	Coulomb kinematic friction; Experimental identification based on standards; Friction coefficients: • steel – steel pairs: 0.25 • steel – laminate pairs: 0.14 • steel – foam pairs: 0.26 • steel – rubber pairs: 0.63 • laminate – rubber pairs: 0.39 • laminate – foam pairs: 0.30 • steel – soil pairs: 0.30 • dry asphalt/concrete – tire pairs: 0.90 • dry roadside – tire pairs: 0.68
Hourglass control	Global stiffness procedure in Flanagan–Belytschko formulation
Displacements	Large
Strains	Large
Numerical integration	Explicit; Finite difference method; Time step assumed based on Courant–Friedrichs–Levy criterion

experimental impact velocities were reduced by 12.3 and 6.3 km/h compared to the standard speed of 110 km/h.

6.2. *Test TB32/CB*

Figs. 4–6 compare the TB32/CB experimental and simulated crash tests, in the form of photos at selected time points, extracted from the video recorded from the top view. Photos of the Dodge Neon car before and after the test are shown in Fig. 7. Fig. 8 compares the relevant graphs of ASI(*t*). The experimental ASI(*t*) curve is shown in two variants:

(1) CAT: a curve determined at the sampling frequency of 10^5 Hz, using DIAdem 2015 software – Crash Analysis Toolkit module;
(2) LPP: a curve determined at the sampling frequency of 10^4 Hz, according to the standard algorithm [1] programmed in the LS-PrePost postprocessor of the LS-Dyna FE code.

Table 5 compares the values of the functionality parameters of barrier SP-05/2 for test TB32/CB. The measured/calculated and rounded (according to standard [2]) values are reported. The conclusions resulting from the full-scale experimental test TB32/CB and from comparison of the simulated and experimental test results are as follows:

(1) In the experimental crash test, the right front (RF) suspension and wheel were destroyed. After the first (major) impact of the car into the barrier, skidding (tail rotation) of the car and rebound of the car from the barrier, with significant crossing of the front line of the exit box were observed.
(2) The reason for the destruction of the RF suspension and wheel could be the age of the car (18 years) and the mileage (~200,000 km). In further tests, cars currently in use should be used.
(3) The experimental ASI(*t*) plot maps the initial impact of the car into the guide rail and successive impacts into seven posts. The first six posts plasticized on contact with the ground, and were overturned on the roadside, after having broken the post-guide rail bolt connections.
(4) The compatibility of the experimental and simulation trajectories of the vehicle motion is good. Slight differences in the trajectories are only observed in the exit box. The main reason could be the lack of criteria for destruction of the RF suspension and wheel in the NCAC car numerical model.
(5) In the initial phase of the collision, the exact value of the ASI parameter in the simulation is higher by 12.0% than that in the experiment (LPP calculations), which is assessed as good compatibility. Qualitative compatibility of the simulation graph ASI(*t*) and the experimental graph is acceptable. The ASI parameter in the simulation corresponds to the impact of the vehicle into the seventh post, causing the skidding and rebound of the car off the barrier. The main reason for this phenomenon could be the lack of criteria for the destruction of the RF suspension and wheel in the NCAC car numerical model.
(6) The oscillations in the simulated ASI(*t*) graph prove too small vibration damping in the NCAC car numerical model. This model requires further modifications on damping and destruction criteria.
(7) The ASI(*t*) graphs calculated by the CAT and LPP algorithms vary slightly, which is caused by reducing the sampling rate by one rank in the LPP algorithm.

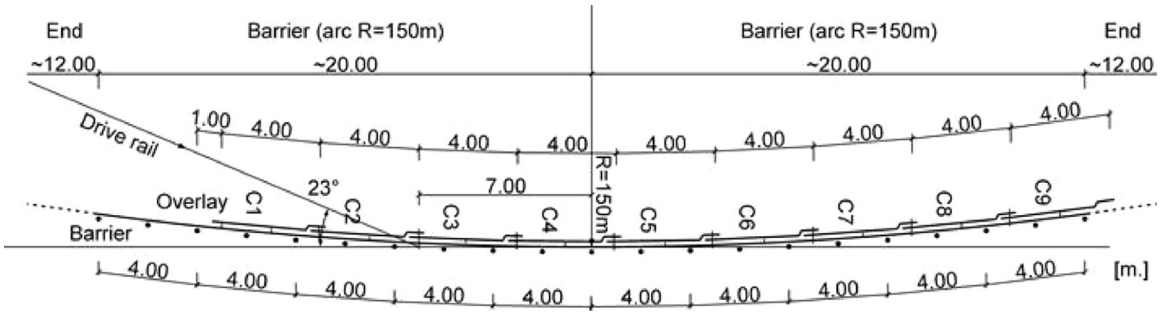

Fig. 3 – Outline of test section of barrier SP-05/2 and sections of overlay CFR2.

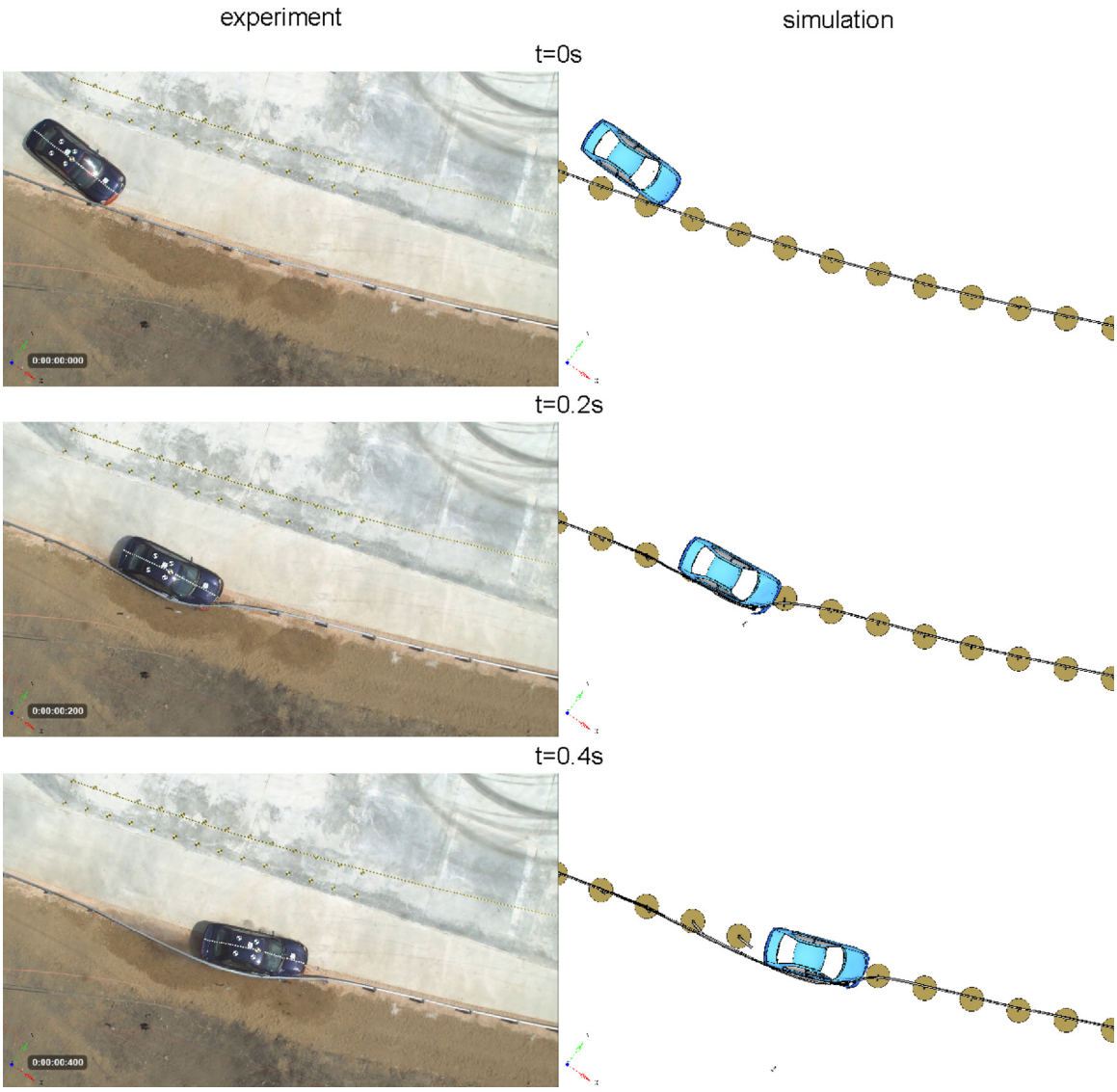

Fig. 4 – Comparison of experimental and simulated tests TB32/CB, from top view, at selected time points (impact velocity v_i = 97.7 km/h). Part 1.

(8) The simulated and experimental values of the THIV parameter are consistent.
(9) The simulated working width is higher by 8.7% than the width in the experiment, which is assessed as good compatibility.
(10) The criteria for approval for the TB32 crash test for a SP-05/2 barrier of class N2-W4-A, built on a horizontal concave arc of a radius of R = 150 m, are met except for the exit box criteria. This conclusion is valid for both the simulation and the experiment.

6.3. *Test TB32/CBC*

Figs. 9 and 10 compare the TB32/CBC experimental and simulated crash tests, in the form of photos at selected time points, extracted from the video recorded from the top view. Photos of the Dodge Neon car before and after the test are shown in Fig. 11. Fig. 12 compares the relevant graphs of the ASI(t). The experimental curve is shown in two variants, CAT and LPP. Table 6 compares the values of the functionality parameters of barrier SP-05/2 for test TB32/CBC. The measured/calculated and rounded (according to standard [2]) values are presented.

The conclusions resulting from the full-scale TB32/CBC experimental test and from comparison of the simulated and experimental test results are as follows:

(1) In the experimental crash test, the RF suspension and wheel were destroyed in a similar manner as in the TB32/CB test. After the major impact of the car into the barrier, a slight rebound of the vehicle off the barrier was observed, redirecting the vehicle towards the barrier followed by next impact at ~1.9 s. The car slipped through the barrier until it

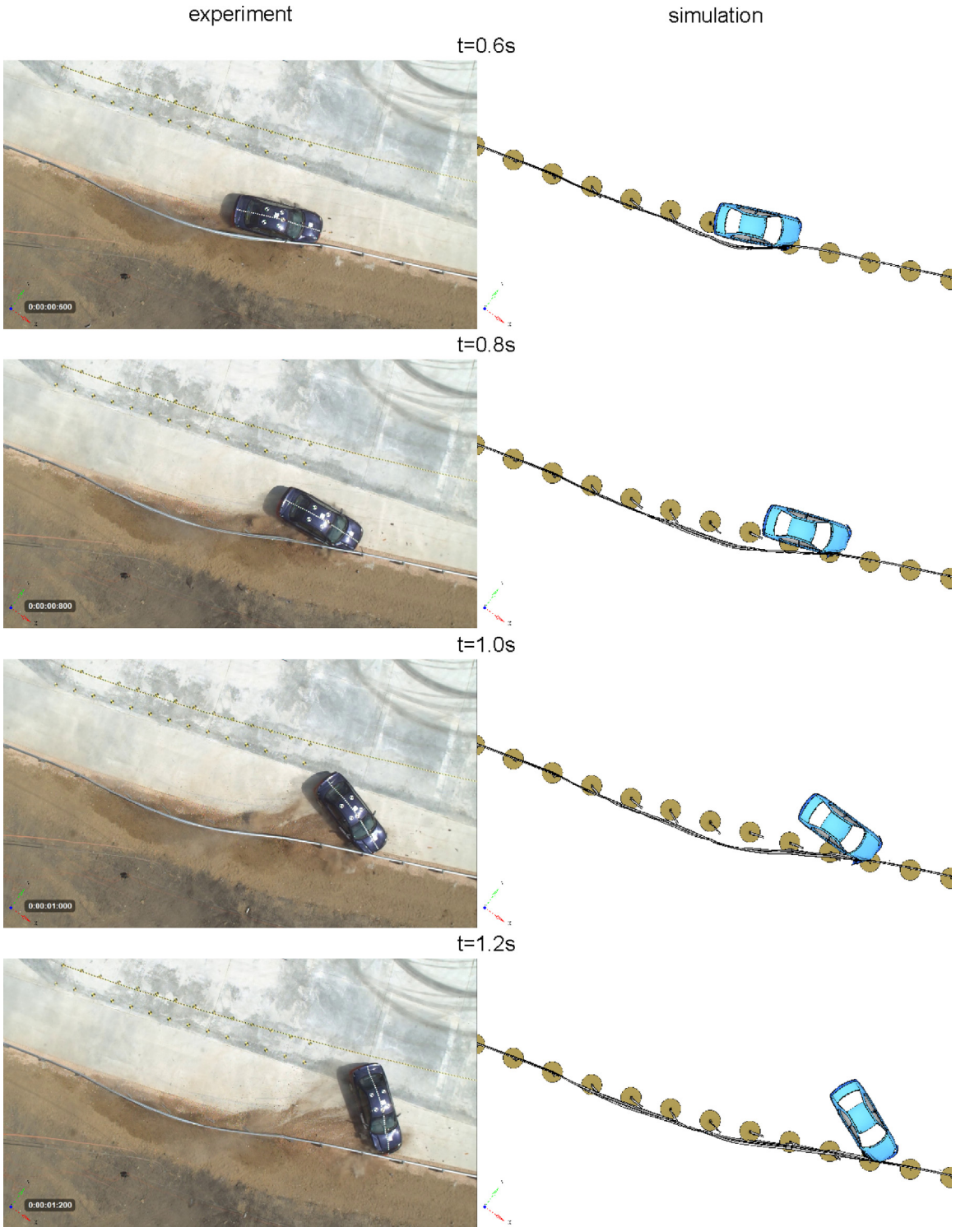

Fig. 5 – Comparison of experimental and simulated tests TB32/CB, from top view, at selected time points (impact velocity v_i = 97.7 km/h). Part 2.

stopped at a distance of ~30 m from the initial theoretical point of impact.

(2) The reason for the destruction of the RF suspension and wheel could be the age of the car (18 years) and the mileage (~200,000 km). In further tests, cars currently in use should be used.

(3) The experimental ASI(t) plot maps the initial impact of the car into the guiderail and successive impacts into five posts which were plasticized and overturned on the roadside, after having broken the post-guide rail screw connections.

(4) The compatibility of the experimental and simulated trajectories of the vehicle motion is good in the time

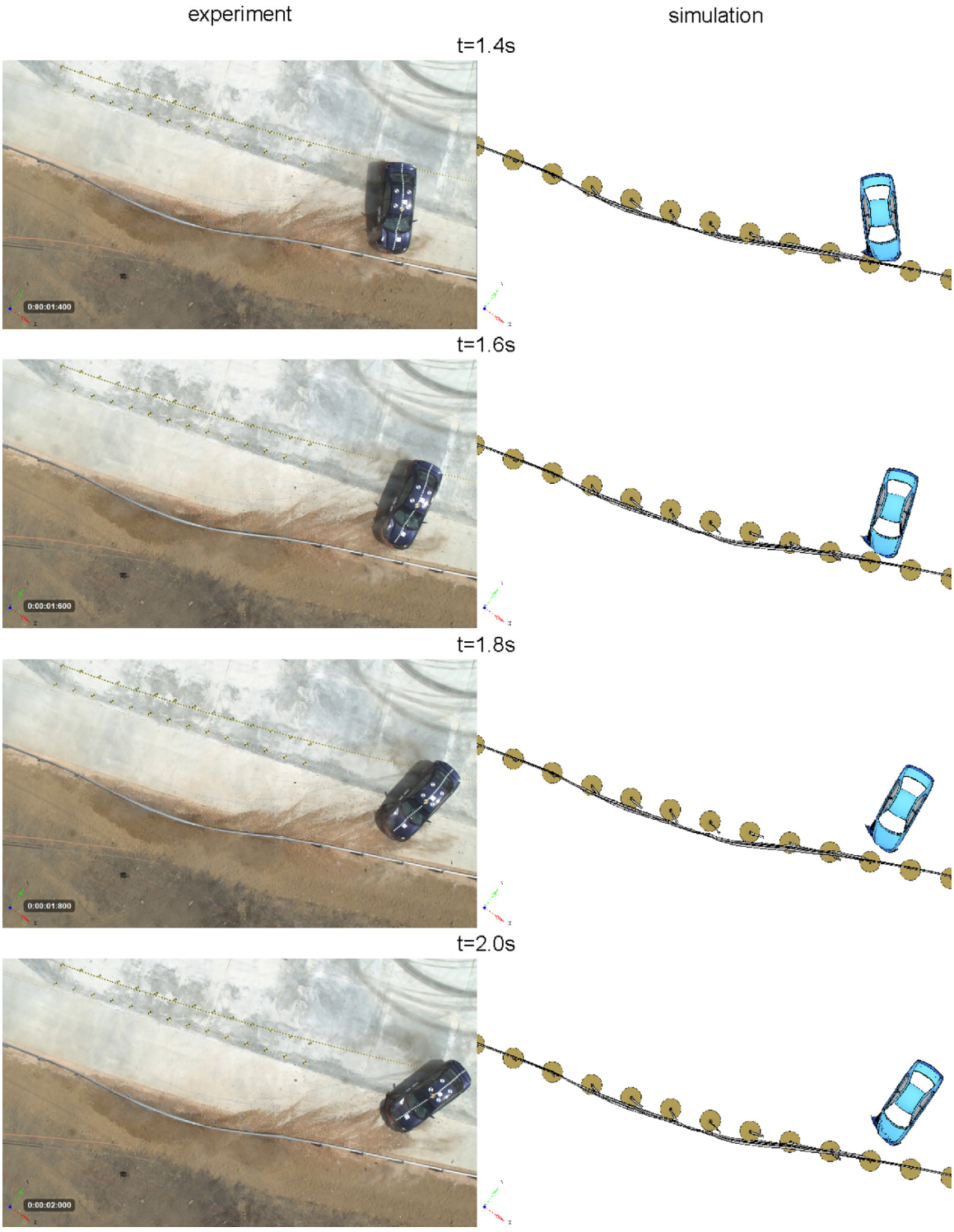

Fig. 6 – Comparison of experimental and simulated tests TB32/CB, from top view, at selected time points (impact velocity v_i = 97.7 km/h). Part 3.

interval [0,0.6] seconds. Considerable differences in the car trajectories are observed after the main impact, after losing contact with the barrier. The main reason for this phenomenon could be the lack of criteria for destruction of the RF suspension and wheel in the NCAC car numerical model.

(5) The simulated ASI parameter value coincides with the experimental value. Qualitative compatibility of the ASI(t) simulated graph and the experimental graph is acceptable. There are visible impacts of the vehicle into successive posts. In the experimental test, six successive posts are hit, whereas the simulated test shows collision with eight

Fig. 7 – Photos of Dodge Neon car used in TB32/CB test.

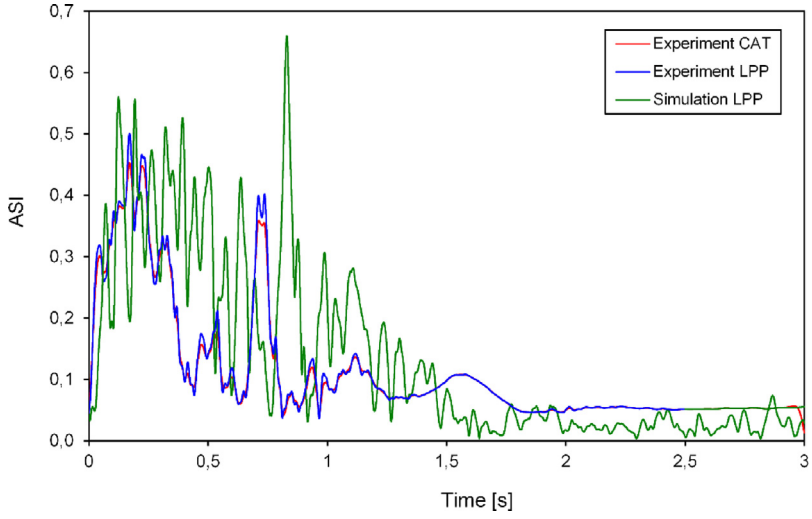

Fig. 8 – Comparison of ASI(t) experimental and simulated graphs for test TB32/CB.

Table 5 – Summary of functionality parameter values of barrier SP-05/2 for test TB32/CB.

Conditions	ASI [–]	THIV [km/h]	W [m]
Experiment, CAT	0.45 (0.5)	16.26 (16)	0.990 (1.0)
Experiment, LPP	0.50 (0.5)	16.30 (16)	
Simulation, LPP	0.56 (0.6 for $t = \sim 0.2$ s)	16.49 (16)	1.076 (1.1)
	0.66 (0.7 for $t = \sim 0.9$ s)		

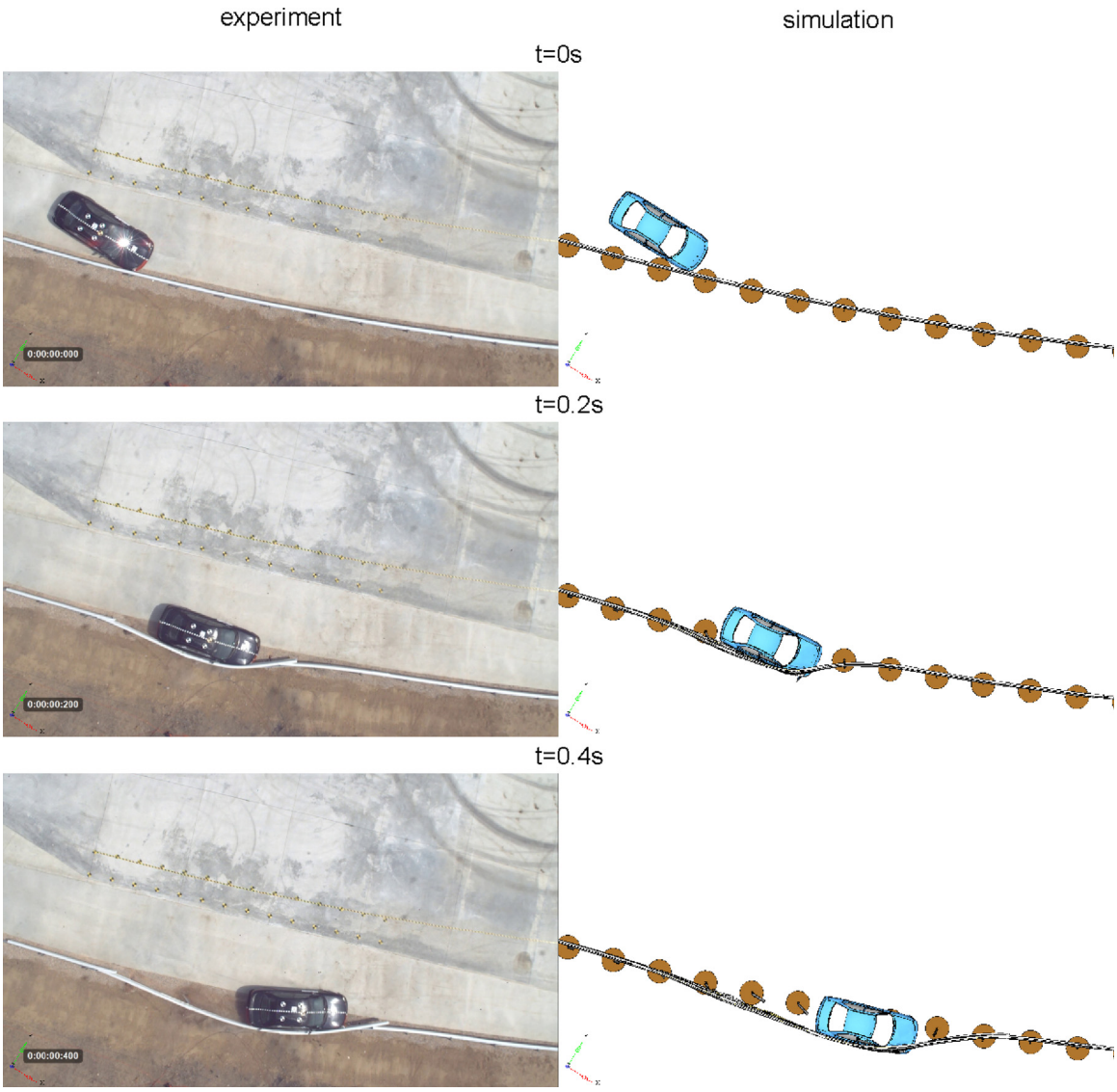

Fig. 9 – Comparison of experimental and simulated tests TB32/CBC, from top view, at selected time points (impact velocity v_i = 103.7 km/h). Part 1.

consecutive posts. The main reason for this phenomenon could be the lack of criteria for the destruction of the RF suspension and wheel in the NCAC car numerical model.

(6) The ASI(t) graphs calculated by CAT and LPP algorithms vary slightly, which is caused by reducing the sampling rate by one rank in the LPP algorithm.

(7) The value of the THIV parameter in the simulation is higher by 11% compared with the experimental value; it is assessed as good compatibility.

(8) The working width W in the simulation is higher by 6.6% than in the experiment, thus it exhibits good compatibility.

(9) The criteria for approval for the TB32 crash test for barrier SP-05/2 of class N2-W4-A, built on a horizontal concave arc of a radius of R = 150 m, are met for both the simulated and experimental tests.

6.4. *Comparison of simulated TB32/CB and TB32/CBC crash tests*

Simulated TB32 crash tests performed on the CB and CBC road restraint systems result in acceptable values of the functionality parameters ASI, THIV and W (Tables 5 and 6). A car trajectory in the exit box is a critical criterion for accepting the TB32 test on a laterally curved barrier. This test is not approved for the CB system because of skidding and rebound of the car from the barrier, with significant crossing of the exit box front line. On the other hand, this test is approved for the CBC system as the car correctly rebounds from the barrier.

Fig. 13 compares the simulated ASI(t) plots corresponding to the both systems. The curve reflecting the behaviour of the TB32/CBC crash test is much lighter compared with the curve for the TB32/CB crash test. Application of the CFR2 overlay results in lowering the ASI value by 35%.

Fig. 10 – Comparison of experimental and simulated tests TB32/CBC, from top view, at selected time points (impact velocity v_i = 103.7 km/h). Part 2.

7. Validation of numerical modelling and simulation of TB32 crash tests with programme RSVVP

The Roadside Safety Verification and Validation Program (RSVVP Rev. 1.3), written in Matlab and accessed in public domain [13], calculates a set of comparison metrics used, among others, in validating roadside safety crash tests and simulations. The metrics are quantitative deterministic mathematical measures of the agreement between two curves. Generally speaking, the comparison metrics calculated by RSVVP can be used to perform a comparison of any pair of curves. The profile 'User selected metric' allows the user to

Fig. 11 – Photos of Dodge Neon car used in TB32/CBC test.

select the desired comparison metrics from the list of 14 different comparison metrics. The comparison metrics are divided into three main categories: MPC (magnitude-phase-composite) metrics, single-value metrics, ANOVA (analysis of variance) metrics.

To compare the simulated and experimental ASI(*t*) curves (test and true curves), the following default metrics assumed in programme RSVVP were evaluated [13]:

(a) MPC metrics: Sprague–Geers Magnitude (*M*), Sprague–Geers Phase (*P*), Sprague–Geers Comprehensive (*C*);

(b) ANOVA metrics: Average of Normalized Residual Errors (*A*), Standard Deviation of Normalized Residual Errors (*D*).

Mathematical definitions of metrics *M*, *P*, *C* are as follows [13]:

$$M = \sqrt{\frac{\sum c_i^2}{\sum m_i^2}} - 1, \quad P = \frac{1}{\pi}\cos^{-1}\frac{\sum c_i m_i}{\sqrt{\sum c_i^2 \sum m_i^2}}, \quad C = \sqrt{M^2 + P^2} \tag{3}$$

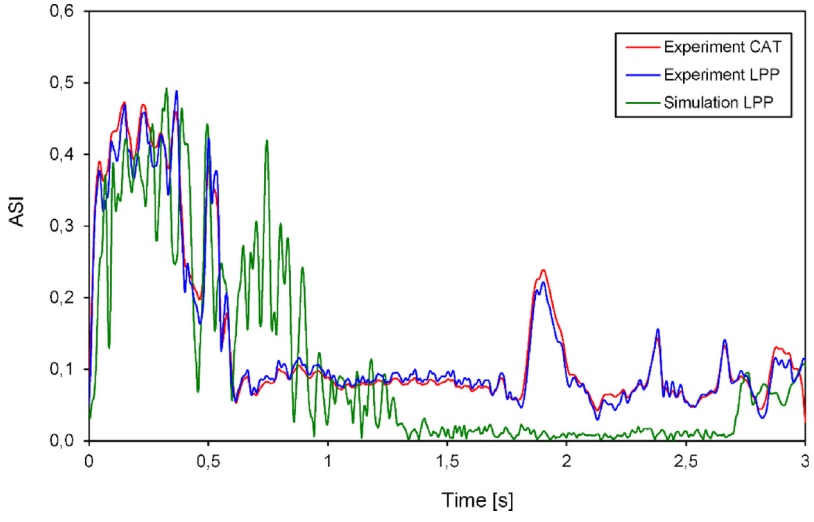

Fig. 12 – Comparison of ASI(*t*) experimental and simulated graphs for test TB32/CBC.

Table 6 – Summary of functionality parameter values of barrier SP-05/2 for test TB32/CBC.

Conditions	ASI [–]	THIV [km/h]	W [m]
Experiment, CAT	0.47 (0.5)	19.77 (20)	1.240 (1.2)
Experiment, LPP	0.49 (0.5)	19.12 (19)	
Simulation, LPP	0.49 (0.5)	21.22 (21)	1.322 (1.3)

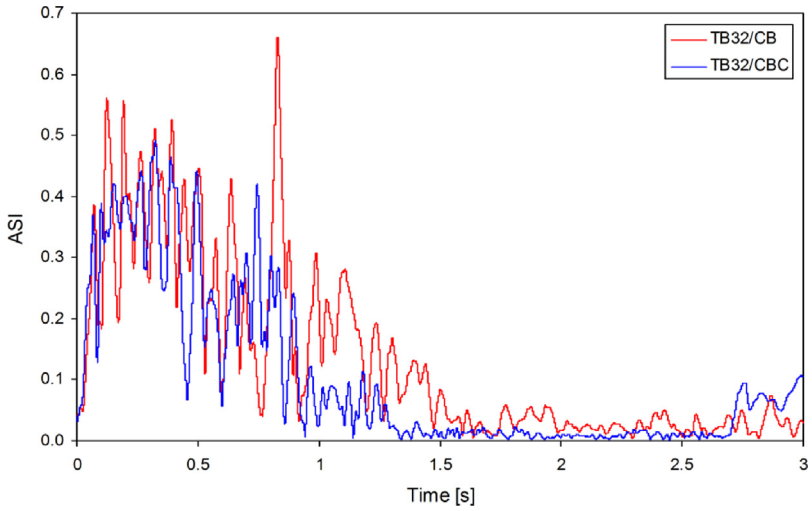

Fig. 13 – Comparison of simulated ASI(t) graphs corresponding to TB32/CB and TB32/CBC crash tests.

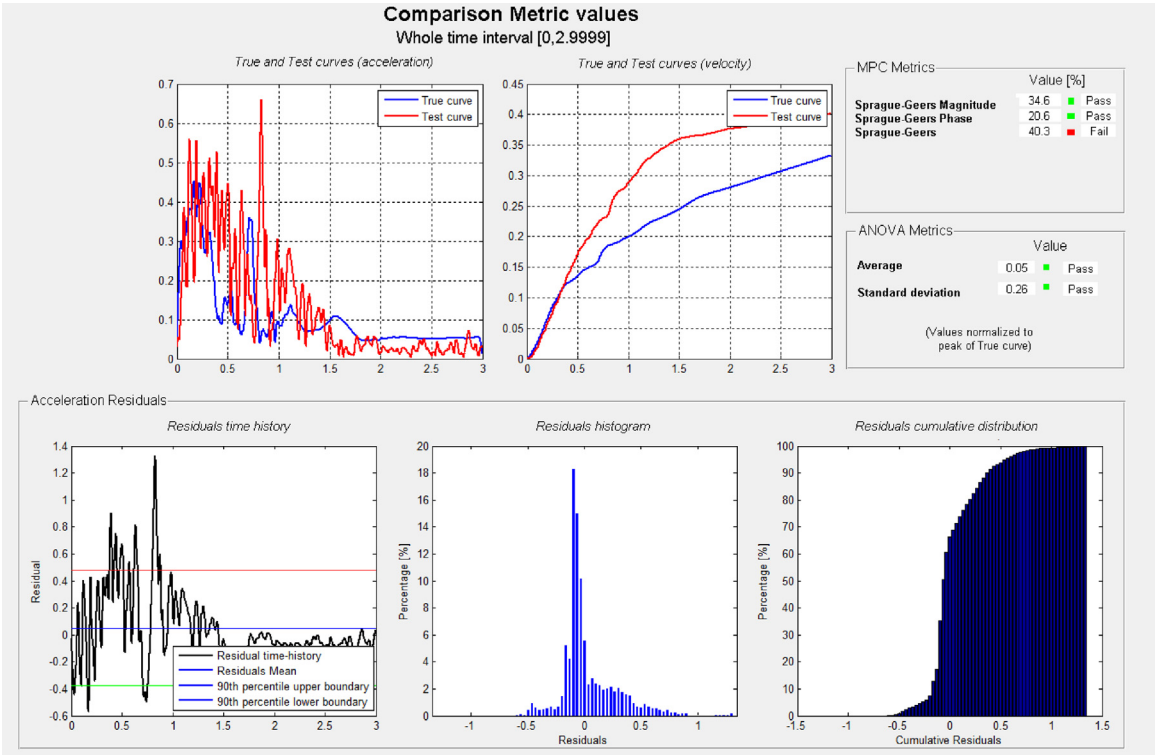

Fig. 14 – Validation of simulated TB32/CB crash test with programme RSVVP.

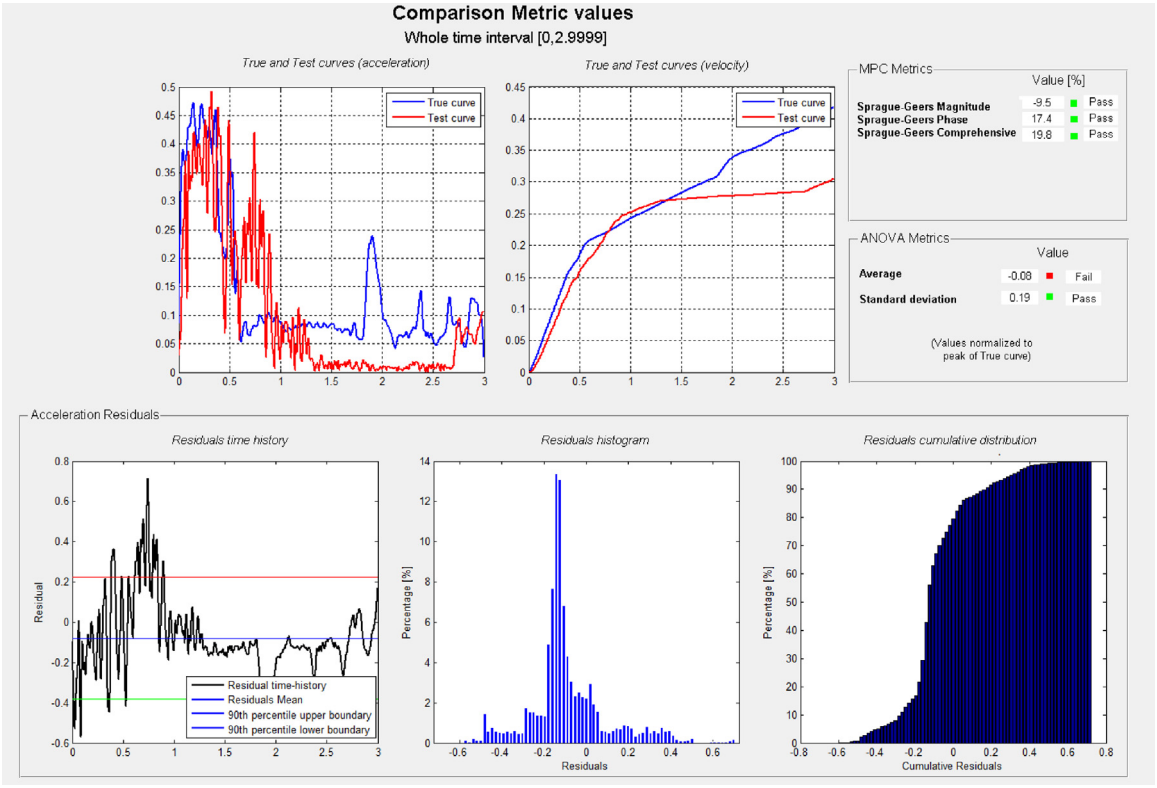

Fig. 15 – Validation of simulated TB32/CBC crash test with programme RSVVP.

The terms m_i and c_i refer to the measured and computed quantities respectively with the "i" subscribe indicating a specific instant in time. According to the NCHRP 22-24 acceptance criteria [13,14], *M*, *P*, *C* should be less than 40%.

Metrics *A*, *D* are related to the ASI(t) normalized residual errors. According to the NCHRP 22-24 acceptance criteria:

(1) the average of residual errors normalized by the peak value of the true curve should be less than 5%;
(2) the standard deviation of the normalized residual errors should be less than 35%.

Apart from the value of the comparison metrics, the cumulative distribution and histogram of the residuals should have the following typical characteristics:

(1) the histogram should have a normal or bell shaped distribution;
(2) the cumulative distribution should have an "S" shape.

Null values, i.e. $M = 0$, $P = 0$, $C = 0$, $A = 0$, $D = 0$, indicate that the two curves are identical.

Figs. 14 and 15 present the results of comparison of the test and true ASI(t) curves, using programme RSVVP, respectively in reference to TB32/CB and TB32/CBC crash tests. The validation passed nearly fully. For TB32/CB test metrics *M*, *P*, *A*, *D* are passed, while metric *C* is failed by 0.3% only compared to the allowable value of 40%. For the TB32/CBC test metrics *M*, *P*, *C*, *D* are passed with a high margin, while metric *A* exceeds the allowable value by 3%. It results from differences between the simulated and experimental cars, described in detail in previous chapters. In both cases the residuals histogram approximately has a normal distribution and the cumulative distribution of an "S" shape.

Despite the differences between the car's numerical model and the old cars used in the full-scale crash tests, the experimental validation of the simulated crash tests with programme RSVVP can be rated positively.

8. Final conclusions

(1) Protective road barriers of class N2-W4-A (B-guiderail, posts interspaced 2.00 m, trapezoidal supporting elements between the guiderail and posts) are widely used in Poland on highways. When these barriers are applied on road bends with a relatively small radius (150 m or so), the exit box criteria in the TB32 crash test may not be met, even at a reduced velocity of the car by about 10% compared to the standard velocity.
(2) In the experimental TB32 crash test for the unmodified road safety barrier of class N2-W4-A, used on a horizontal concave arc of a 150 m radius, the front right suspension and wheel of the car were destroyed. After the major impact of the car into the barrier, skidding of the vehicle and rebound of the vehicle off the barrier, with substantial crossing of the front line of the exit box were observed.

(3) The use of the protective composite-foam overlay CFR2, combined with a B-type guiderail, is one of possible design solutions to ensure approval for the TB32 crash test in the conditions specified in conclusion (2).
(4) The possible reason for destruction of the FR suspension and wheel of the Dodge Neon car used in the experiments could be the car's age (18 years) and mileage (~200,000 km). In further TB32 tests, cars of different makes currently in use, weighting 1500 kg should be applied.
(5) The experimental verification of the TB32 simulation crash tests, for the selected curved barrier without and with the CFR2 protective overlay, is reasonably positive. The comparison includes ASI(t) graphs, ASI values, THIV values, working width values and car motion trajectories. The main reason for some differences between the experiment and the simulation could be the lack of criteria for destruction of the RF suspension and wheel in the NCAC numerical model of a Dodge Neon car. The NCAC car numerical model requires further modifications related to destruction criteria and vibration damping.

Ethical statement

Authors state that the research was conducted according to ethical standards.

Acknowledgements

This work was supported by the grant from the National Centre for Research and Development, Poland [Grant Number PBS1/B6/14/2012]. Proofreading of the article was provided Mrs. Christine Frank-Szarecka, Canada.

REFERENCES

[1] European Standard EN 1317-1:2010. Road Restraint Systems – Part 1: Terminology and General Criteria for Test Methods, 2010.
[2] European Standard EN 1317-2:2010. Road Restraint Systems – Part 2: Performance Classes, Impact Test Acceptance Criteria and Test Methods for Safety Barriers Including Vehicle Parapets, 2010.
[3] European Standard EN 1317-5:2007+A2:2012. Road Restraint systems – Part 5: Product Requirements and Evaluation of Conformity for Vehicle Restraint Systems, 2012.
[4] M. Klasztorny, D.B. Nycz, P. Szurgott, Modelling and simulation of crash tests of N2-W4-A category safety road barrier in horizontal concave arc, Int. J. Crashworthiness 21 (6) (2016) 644–659.
[5] Z. Ren, M. Vesenjak, Computational and experimental crash analysis of the road safety barrier, Eng. Fail. Anal. 12 (2005) 963–973.
[6] M. Borovinsek, M. Vesenjak, M. Ulbin, Z. Ren, Simulation of crash tests for high containment levels of road safety barriers, Eng. Fail. Anal. 14 (2007) 1711–1718.
[7] P. Dziewulski, Examination of Selected Structures to Improve Energy Intensity of Road Safety Barriers, (Ph.D. Thesis, in Polish), Military University of Technology, Warsaw, Poland, 2010.
[8] System N2-W4-A (SP-05/2), Stalprodukt S.A., Bochnia, Poland, 2011.
[9] Vehicle Models, National Crash Analysis Center, USA, http://www.ncac.gwu.edu/vml/models.html (accessed 07.01.13).
[10] Crash Simulation Vehicle Models, National Highway Traffic Safety Administration, USA, https://www.nhtsa.gov/crash-simulation-vehicle-models (accessed 20.07.17).
[11] J.O. Hallquist, LS-DYNA Keyword User's Manual, Livermore Software Technology Corporation, USA, 2007.
[12] PN-ISO 10392:1997. Road Vehicles With Two Axles – Determination of Centre of Gravity, 1997 (in Polish).
[13] M. Mongiardini, M.H. Ray, Roadside Safety Verification and Validation Program (RSVVP). User's Manual, Rev. 1.3, Worcester Polytechnic Institute, USA, 2009.
[14] NCHRP 22-24. Guidelines for Verification and Validation of Crash Simulations Used in Roadside Safety Applications, Worcester Polytechnic Institute, USA. http://apps.trb.org/cmsfeed/TRBNetProjectDisplay.asp?ProjectID=697 (31.01.11).